

# Controlling QCLs for frequency metrology from the infrared to the THz range

Luigi Consolino, Francesco Cappelli, Michele De Regis, Giulio Campo, Iacopo Galli, Davide Mazzotti, Pablo Cancio, Simone Borri, Giovanni Giusfredi, Saverio Bartalini, Paolo De Natale  
Istituto Nazionale di Ottica, CNR-INO, Largo E. Fermi, 6 Firenze, Italy

## ABSTRACT

The Quantum Cascade Laser is becoming a key tool for plenty of applications, from the IR to the THz range. Progress in nearby areas, such as the development of ultra-low loss crystalline microresonators, optical frequency standards and optical fiber networks for time&frequency dissemination, are paving the way to unprecedented applications in many fields. For the most demanding applications, a thorough control of quantum cascade lasers (QCLs) emission must be achieved. In the last few years, QCLs unique spectral features have been unveiled, while multifrequency, comb-like QCLs have been demonstrated. Ultra-narrow frequency linewidths are necessary for metrological applications, ranging from cold molecules interaction and ultra-high sensitivity spectroscopy to infrared/THz metrology. In our group, we are combining crystalline microresonators, with a combined high quality factor in the infrared and ultra-broadband spectral coverage, with QCLs and other nonlinear highly coherent and frequency referenced sources. Frequency referencing to optical fiber-distributed optical primary standards offers astonishing stability values of  $10^{-16}$  @1-sec timescales in laboratory environments but several hundred kilometres far away from the primary clocks. A review will be given of the present status of research in this field, with a view to perspectives and future applications.

**Keywords:** Quantum Cascade Lasers, Frequency Metrology, Microresonators

## 1. INTRODUCTION

One of the most significant developments for semiconductor physics, in recent years, has been the development of a new class of emitters based on intersubband transitions. These devices have attracted considerable interest from the viewpoint of fundamental physics and, nowadays, have achieved a considerable impact in real world applications. In 1971, Kazarinov and Suris<sup>1</sup> first proposed the use of intersubband transitions for radiation amplification in a superlattice structure. Since then, the birth and development of growth techniques, such as molecular beam epitaxy (MBE)<sup>2</sup>, with unprecedented control on layer thickness, has disclosed the way to the design of new materials by semiconductor bandgap engineering<sup>3</sup>. In this context, the possibility to use heterostructures to modulate the bandgap, creating sharp discontinuities in the conduction and valence bands, has allowed the investigation of a new class of phenomena and devices.

In this framework, Quantum Cascade Lasers (QCLs)<sup>4,5</sup> can be considered the primary achievement of electronic band structure engineering, showing how artificial materials can be created through quantum design to have tailor-made properties. QCLs are unipolar devices exploiting optical transitions between electronic states (conduction subbands) created by spatial confinement in semiconductor multi-quantum-wells. The QCL has a ground-breaking design based on the engineering of electronic wavefunctions on a nanometer scale. As far as the macroscopic properties of materials are defined by their electronic structure, the QCL is based on an artificial nano-material. The extreme precision of the material growth that is required to get the proper operation properties, combined with the large number of layers and the complexity of the structure, gives an impressive demonstration of the capabilities offered by bandgap engineering, and can be used to explore and implement novel quantum physical parameters.

Heterostructure lasers operating in the visible and near-IR range have proven crucial to foster applications in plenty of fields, including information and communication technologies. On the other hand, the development of Quantum Cascade Lasers, semiconductor lasers able to cover the wide mid-infrared (mid-IR)/far-infrared (far-IR) regions of the electromagnetic spectrum, have allowed to fill the gap due to the limitations of other sources, like OPOs, CO<sub>2</sub>, Ti:sapphire, or lead salt lasers, thus significantly extending the range of use of compact semiconductor sources. Since their first demonstration, QCLs operating in the mid-IR have undergone an impressive development, achieving high performance levels. For example, in pulsed mode, the maximum operating temperature can be even higher than room

temperature in a wide range of wavelengths (5–12  $\mu\text{m}$ ). Significantly, room-temperature continuous-wave (CW) single-mode operation around 9  $\mu\text{m}$  has been demonstrated.<sup>6</sup> Multi-watt output power, continuous wave, room temperature devices operating across the mid-IR, with wallplug efficiencies larger than 50%, have been recently reported<sup>7,8</sup>, with impressive performances in terms of spectral coverage ( $\sim$ 3–25  $\mu\text{m}$ ) and tunability range.<sup>9</sup> QCLs with new promising material systems have been recently demonstrated to work up to 400 K at wavelengths within the first atmospheric window (3–5  $\mu\text{m}$ )<sup>10,11</sup>. In 2002, the spectral coverage of QC sources was extended to the far-IR,<sup>12</sup> where efficient and miniaturized sources operating in the 1.2–4.9 THz window have now been successfully developed, in either single plasmon<sup>5</sup> or double-metal waveguide configuration.<sup>12</sup>

A peculiar feature of QCLs is the possibility to tune the emission frequency over a large bandwidth without changing the semiconductor material system, by changing the size of quantum wells to vary the energy separation of electronic states. This distinctive characteristic, together with the unipolar nature of the charge transport and the peculiar shape of the density of states, enables features totally different from those of bipolar lasers, that have an emission wavelength depending on the material bandgap and having a gain strongly temperature dependent. Moreover, in contrast with conventional interband semiconductor lasers, in a QCL the gain linewidth depends only indirectly on the temperature, and the optical gain is not limited by the joint density of states. This leads to the absence of gain saturation when electron and hole quasi-Fermi levels are well within conduction and valence bands. The gain is therefore only limited by the amount of current that can be driven in the structure to sustain the population in the upper state. In addition, the multistage cascaded geometry allows for electron recycling, so that each electron injected above threshold may generate a number of photons equal to the number of stages. The cascade geometry has the significant advantage that a uniform gain across the active region is limited by the ratio of the effective transit times between wells, including capture of the slower carrier and recombination times. The number of stages is mostly limited by the ratio between the effective width of the optical mode and the length of an individual stage.

The tremendous progress these sources have undergone in the last decades has been possible thanks to a thorough characterization of these devices, e.g. unveiling their unique spectral features. Indeed, extremely narrow frequency linewidths, at tens of Hz or below, are necessary for demanding applications, ranging from cold molecules interaction<sup>13,14</sup> and ultra-high sensitivity spectroscopy<sup>15</sup> to infrared/THz metrology.<sup>16,17</sup> Towards these goals, complete characterization and control of the emission of QCL is necessary. In fact, though QCLs have shown extremely high spectral purity both in the mid-IR and in the THz domain, a crucial step towards an extensive use of QCLs for demanding spectroscopic and metrological applications is the development of techniques enabling not only the narrowing of the QCL emission down to the kilohertz level but also its referencing to a stable frequency standard. These opportunities will be discussed in details not only for already available mid-IR devices and THz QCLs, but also for new generation sources that are arising as the new frontiers of unipolar devices, including mid-IR QCL combs and room-temperature THz QCLs.

## 2. MID-IR QCLS

### 2.1 Single-frequency Mid-IR QCLs stabilization and spectroscopy

To perform high-sensitivity and high-resolution sub-Doppler spectroscopy in the mid infrared, it is necessary the availability of intense and narrow (low-frequency-noise) laser sources. Moreover, if also a high accuracy is required, i.e. control on systematic uncertainties, an absolute reference for frequencies is needed. QCLs are ideal candidates for this role, since their intrinsic linewidth is comparable to the natural linewidth of molecular transitions (tens–hundreds of Hz), and the emitted radiation intensity spans from the milliwatt up to the watt level. Moreover, their tunability is another desirable feature. Unfortunately, on a time scale spanning from 1 s to 10 ms, QCLs linewidth is way wider in free-running operation (about 1 MHz) due to the  $1/f$  noise contribution. Two main approaches can be used in order to overcome this limitation and to provide the desired absolute frequency reference: (1) The QCL emission can be stabilized and narrowed against a molecular absorption line, (2) or it can be referenced to an optical frequency comb (OFC) through a phase-locking chain. Such schemes are here described.

#### 2.1.1 Polarization locking

With the following experiment, a method to obtain a narrow-emission and absolutely-referenced QCL has been proven.<sup>18</sup> It exploits the availability of a natural ruler of frequency references given by the many strong molecular absorption lines, whose center frequency can be absolutely measured with a sub-kHz precision.<sup>19</sup> Basing on this, it is possible to have a simple system for high-sensitivity/precision spectroscopy for a specific molecular species, without using an OFC. A polarization-spectroscopy (PS) scheme produces, without any external modulation, the narrow dispersive sub-Doppler

signal used to close the feedback loop on the QCL driving current for frequency stabilization. It will be shown that the linewidth of a continuous-wave room temperature QCL can be narrowed below 1 kHz (FWHM) by locking the laser to a CO<sub>2</sub> line. The laser is a room temperature DFB QCL emitting at 4.3 μm, provided by Hamamatsu Photonics. It is operated at a temperature of 283 K and a current of 710 mA, delivering an output power of about 10 mW. A schematic of the experiment is shown in fig. 1. The QCL is mounted on a specific compact thermoelectrically-cooled mounting. A low-noise home-made current driver is used. It ensures a current noise power spectral density always below 1nA/√Hz, while keeping a fast current modulation capability, thanks to a control circuitry placed in parallel to the QCL based on a field-effect transistor (FET).

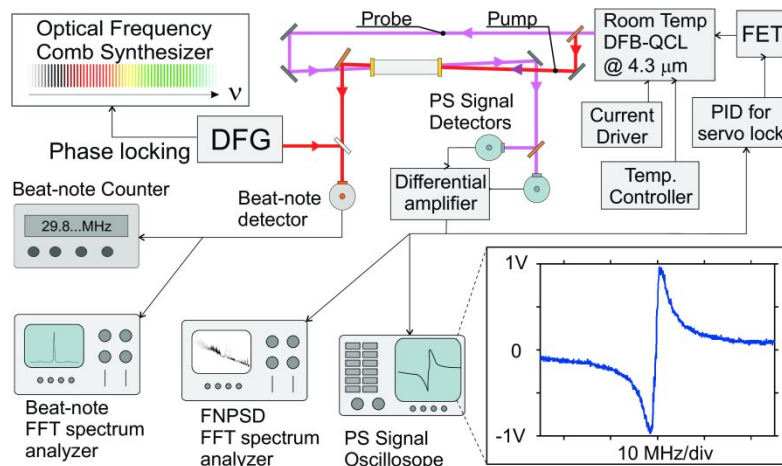


Figure 1. Polarization-locking setup. The probe beam gives the signal used for the frequency locking. The pump beam is also used for the beat-note detection and the frequency counting. PS: polarization spectroscopy, DFG: comb-referenced single-frequency difference-frequency generation, FET: field-effect transistor, FFT: fast Fourier transform. Reprinted with permission from [18], copyright 2012.

The chosen molecular transition is the P(29)e of the (01<sup>1</sup>1 – 01<sup>1</sup>0) ro-vibrational band of CO<sub>2</sub> at 2311.5152 cm<sup>-1</sup> (see section 1.1.3). The inset of fig. 1 shows a typical scan of the PS signal at a pressure of 8.9 Pa, when the laser frequency is tuned across the molecular resonance. By carefully balancing the differential detection, a zero-offset signal is obtained. It ensures a linear conversion of the laser frequency fluctuations into amplitude variations in the region centered around the resonance frequency. For the QCL frequency stabilization, the PS signal is processed by a home-made PID controller, and fed back to the FET gate for current control. From a preliminary analysis of the free-running frequency noise power spectral density (FNPSD) of a similar QCL,<sup>20</sup> it is expected that a locking bandwidth of about 100 kHz is required for reaching a kHz-level linewidth. In order to ensure this condition, both the differential amplifier and the PID have been designed to have bandwidths larger than 1 MHz. However, there are two more fundamental aspects that can limit the loop bandwidth. The first is the roll-off of the QCL tuning rate with the modulation frequency:<sup>21</sup> the tuning rate is never flat, even at low frequencies, and shows a -3 dB cut-off at about 100 kHz. The second is the width of the linear region of the PS signal, that introduces a frequency roll-off starting from 300 kHz. Following the above considerations, the bandwidth of the frequency-locking loop is expected to be in the range of a few hundred kHz.

In order to characterize the frequency locking, two different measurements are carried out in parallel. The first one is the spectral analysis of the in-loop PS signal, the second one is the analysis of the beat note between the QCL and a narrow OFC-referenced DFG source providing a stable (10-Hz linewidth within 100 μs) and absolute reference. Each measurement has been also performed with the QCL in free-running regime.

In fig. 2-left the FNPSD measurement results are shown. Firstly, it is noteworthy to highlight the improvements in the free-running regime brought by the evolution of the current driver: using the new-generation low-noise driver, the FNPSD exhibits a clean 1/f trend, confirming that virtually no external noise is added. By closing the frequency-locked loop, the FNPSD is reduced in the spectral range below 250 kHz, which is then assumed to be the loop bandwidth, as expected. At about 450 kHz, the onset of a self-oscillation peak is evident. It can be well explained by the dephasing introduced by the approaching roll-offs mentioned above and it is, at present, the factor limiting the loop performances.

The FNPSD of the locked QCL is obtained by adding to the closed-loop error signal the detection noise floor. The latter is dominated, in the low-frequency range, by the residual intensity noise of the QCL, and limits the frequency-noise reduction. The effect of the locking on the QCL emission line shape can be more intuitively described by the spectrum of the beat note between the QCL radiation and the DFG one. An acquisition is shown in fig. 2-right. The 450 kHz servo bumps confirm the oscillation peak appearing in the FNPSD.

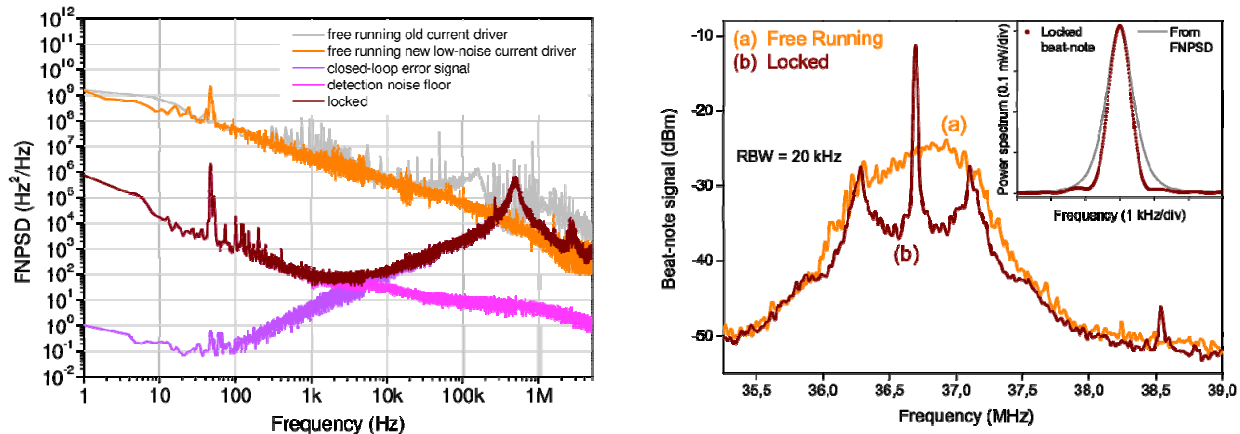


Figure 2. **Left:** Comparison between the free-running QCL FNPSDs and the locked one. The locked QCL FNPSD is obtained by summing the spectrum of the closed-loop error signal to the PS detection noise floor, measured with empty gas cell. **Right:** FFT spectra of a 10-ms-long evolution of the beat note between the QCL, in free-running (trace a) and locked (trace b) conditions, and the narrow DFG source. Inset: zoomed view (linear scale) of the central peak observed over 1 ms with a resolution bandwidth of 721 Hz (dotted curve) and QCL power spectral profile retrieved from the locked FNPSD (straight line). Reprinted with permission from [18], copyright 2012.

By comparing the areas of the locked and free-running beat notes we obtain that 77% of the QCL radiation power is forced into the narrow peak centered on the molecular line. Switching from the free-running to the locked regime the linewidth (FWHM) is reduced from about 500 kHz down to 760 Hz on a 1-ms time scale (inset). The inset also shows the comparison between the beat note and the locked QCL power spectral profile retrieved from its FNPSD over a 1 ms time scale. For the latter, a 900 Hz FWHM is obtained, in good agreement with the beat-note linewidth. The beat-note frequency is also measured by a 1-s-gated frequency counter over about 2 hours. The obtained Allan deviation<sup>22</sup> is 3 kHz at 1 s and decreases down to 0.9 kHz up to 320 s. Then, for longer times, it increases again, due to slow variations of the locking signal offset. This prevents our oscillator from achieving the stability performances of the best mid-infrared standards.<sup>23</sup> The absolute frequency of the CO<sub>2</sub> line is measured by averaging a set of frequency counts performed counting in several days the beat note, and knowing the DFG frequency thanks to the reference. The obtained value is (69297480.708 ± 0.025) MHz, with an uncertainty which takes into account both the repeatability of the offset zeroing and the OFC accuracy. This result is in agreement with the value given by HITRAN database<sup>24</sup> for this transition, but with at least 2 orders of magnitude increased accuracy.

### 2.1.2 Single-frequency phase locking

Direct phase locking of QCLs to OFCs is a valid alternative respect to frequency locking to a molecular absorption line, allowing to enhance the frequency stability while preserving the full tunability of the laser source, at the cost of a more complex and bulky setup.

In the scheme here presented the QCL is directly phase-locked to a DFG mid-infrared radiation obtained starting from two OFC-referenced near-infrared sources.<sup>25</sup> This method provides simultaneously an absolute frequency reference and a residual phase noise independent of the OFC noise. A final QCL narrowing below the OFC tooth linewidth is obtained: indeed, a linewidth below 1 kHz on a 1 ms time scale is obtained from the analysis of the FNPSD. The QCL frequency stability and the absolute traceability have been characterized, resulting both limited by the Rb-GPS-disciplined 10-MHz quartz oscillator reference of the OFC. Precision and high resolution spectroscopy performances of this QCL source are tested by measuring the frequency of the saturation Lamb dip of few CO<sub>2</sub> transitions with an uncertainty of  $2 \times 10^{-11}$ .

The laser is a room temperature distributed-feedback QCL emitting at 4.3  $\mu\text{m}$ . It is operated at a temperature of 283 K and a current of 710 mA. The radiation which the QCL has been locked to is produced by non-linear DFG process in a periodically-poled LiNbO<sub>3</sub> crystal<sup>26</sup> by mixing an Yb-fiber-amplified Nd:YAG laser at 1064 nm and an external-cavity diode laser (ECDL) emitting at 854 nm. The peculiar locking scheme, employing a direct digital synthesis (DDS) technique,<sup>27,28,29</sup> makes the ECDL be effectively phase-locked to the Nd:YAG laser, while the OFC just acts as a transfer oscillator adding negligible phase noise to the DFG radiation. As a consequence, the mid-infrared radiation is referenced to the Cs frequency standard through the OFC, but its linewidth is independent of the OFC one.

A schematic of the experimental setup is shown in fig. 3. A small portion of the QCL beam, taken with a beam-splitter, is used for the phase-locking. It is overlapped to the DFG beam through a second beam splitter and sent to a 200-MHz-bandwidth HgCdTe detector. A 100-MHz beat note is detected by using few  $\mu\text{W}$  of both QCL and DFG sources. The beat note is processed by a home-made phase-detection electronics, which compares it with a 100-MHz local oscillator (LO) and provides the error signal for closing the phase-locked loop (PLL). A home-made PID electronics processes the error signal and sends it to the gate of a field-effect transistor (FET) to fast control the QCL driving current.

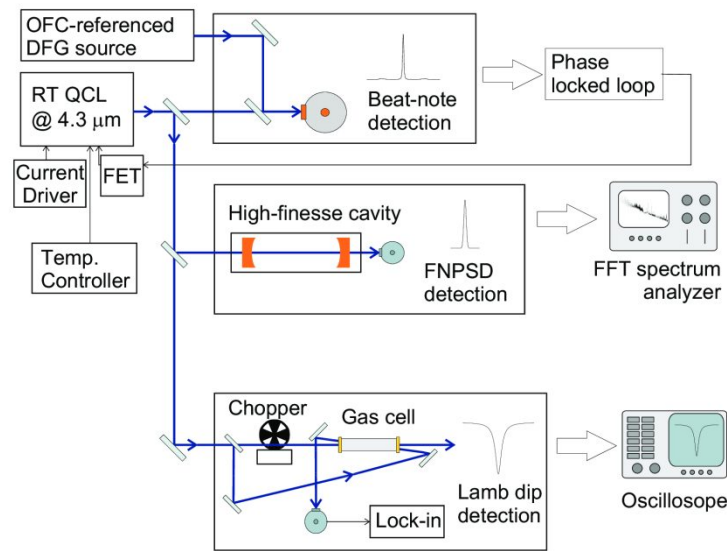


Figure 3. Schematic of the experimental setup. There are three main parts: the beat-note detection between QCL and DFG for the phase-locking, the high-finesse cavity for FNPSD analysis and the saturation spectroscopy signal detection for the absolute frequency measurement of the CO<sub>2</sub> transitions. Reprinted with permission from [25], copyright 2013.

In fig. 4-left the beat note acquired using a FFT spectrum analyzer is shown. The width of the carrier frequency is limited by the instrumental resolution bandwidth, as expected from a beat note between two phase-locked sources. The locking bandwidth is limited by the dependence of the QCL tuning rate on the modulation frequency. A 250-kHz locking bandwidth is achieved, as confirmed by the servo bumps in the beat note. The phase-locking performance in terms of residual RMS phase error is measured by using the fractional power  $\eta$  contained in the coherent part of the beat-note signal, i.e. in the carrier. By evaluating the ratio between the area under the central peak of the beat note and the area under the whole beat-note spectrum (1.5-MHz wide), a phase-locking efficiency of  $\eta = 73\%$  is obtained, yielding a residual RMS phase noise of 0.56 rad. The main portion of the QCL radiation is used for frequency-noise characterization and for spectroscopy. To the first purpose the QCL beam is coupled to a high-finesse cavity, which works as frequency-to-amplitude converter, when its length is tuned in order to have a transmission corresponding to half the peak value. The cavity free spectral range is 150 MHz, and its finesse is about 9000 at  $\lambda = 4.3 \mu\text{m}$ , as measured with the cavity-ring-down technique, leading to a mode FWHM of 18.8 kHz. The cavity output beam is detected by a second HgCdTe detector, and the resulting signal is processed by a FFT spectrum analyzer.

In fig. 4-right the FNPSD of the phase-locked QCL, acquired by using the high-finesse cavity, is shown. The same cavity has been also used to measure the DFG FNPSD and the QCL FNPSD when frequency-locked to a molecular absorption line. Such an independent converter allows for a fair comparison between the two basically different locking techniques. The plotted FNPSDs are compensated for the high-frequency cavity cut-off, due to the photon cavity ring-down rate ( $f_c = 9.4$  kHz). The free-running QCL FNPSD, recorded by using the slope of the Doppler broadened CO<sub>2</sub> absorption line as converter, is shown.

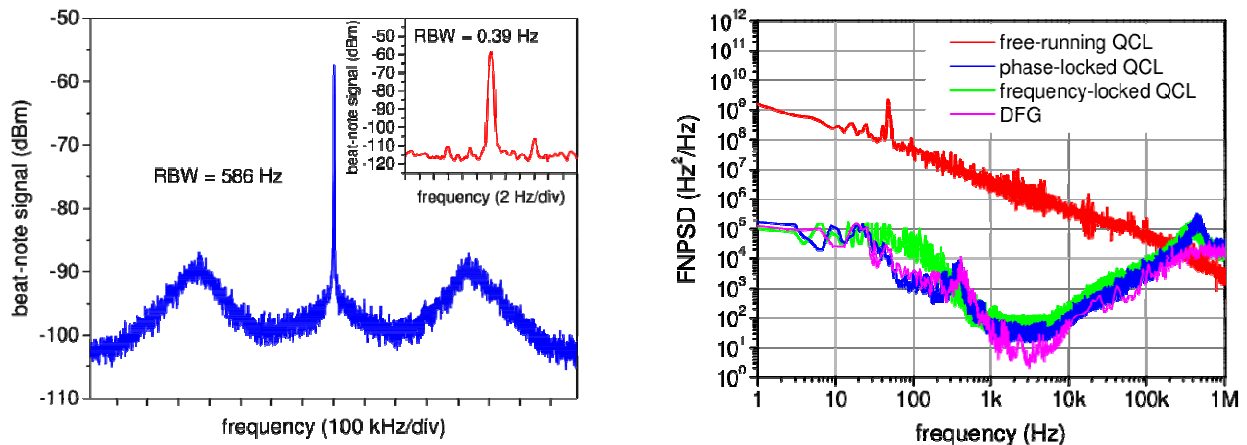


Figure 4. **Left:** Beat-note signal between the DFG radiation and the phase-locked QCL. The inset shows the same beat note with a narrower span and resolution bandwidth. In both cases the width of the peak (FWHM) is limited by the resolution bandwidth of the spectrum analyzer. **Right:** QCL FNPSDs in free-running and phase-locked conditions, acquired by using a CO<sub>2</sub> line and the high-finesse cavity as frequency-to-amplitude converters, respectively. Reprinted with permission from [25], copyright 2013.

The comparison between free-running and phase-locked conditions confirms a locking bandwidth of 250 kHz, with a frequency noise reduction of about four orders of magnitude for frequencies up to 10 kHz. Moreover, the phase-locked-QCL FNPSD perfectly overlaps the DFG one, with only an excess noise above 200 kHz. If we compare the QCL FNPSD when phase/frequency locked to the DFG/molecular transition, they are almost coincident for Fourier frequencies above 1 kHz up to 450 kHz where a self-oscillation of both control loops is observed. This confirms that the locking bandwidth is limited by the laser modulation bandwidth. Nevertheless, a QCL linewidth narrower than 1 kHz (FWHM) on a time scale of 1 ms is retrieved in both cases by integrating the FNPSDs for frequencies above 1 kHz. As a consequence, we note that phase-locking the QCL does not improve laser narrowing with respect to frequency-locking. On the other hand, between 30 Hz and 1 kHz the two curves show different trends: in this range the phase-locked QCL FNPSD lies below that of the frequency-locked one, except for an evident noise peak centered at 400 Hz, which is also present in the DFG source. Apart from this peak, the comparison in this frequency range confirms a better control of the frequency jitter for the phase-locked QCL, overcoming the limits of the frequency-locked QCL set by the presence of a residual amplitude noise. For Fourier frequencies below 30 Hz the high-finesse cavity is no more a good frequency-to-amplitude converter, since it saturates.

### 2.1.3 Stabilization with crystalline whispering gallery mode resonators

An alternative effective tool for laser stabilization and linewidth narrowing is represented by high-Q whispering gallery mode resonators (WGMR). WGM resonators made of crystalline materials have started to be used for mid-IR applications in the last couple of years. They are particularly interesting because of their potential to achieve high optical quality (Q) factors (up to 10<sup>11</sup> in the near IR<sup>30</sup>) as well as to cover a wide transparency range, from the uv to the mid-IR. The ultimate Q factors of the modes are determined by the intrinsic material loss and scattering. The very sharp frequency response of resonant modes make WGMRs appealing for sensing applications. Moreover, thanks to their narrow mode widths, crystalline WGMRs are attractive for frequency reference applications.

In our work, we studied complementary methods for stabilization of a QCL emitting at 4.3  $\mu\text{m}$  wavelength, including all-electronic locking onto the transmission and reflection modes of the resonator.<sup>30</sup> We used a CaF<sub>2</sub> toroidal WGMR

from OE waves. The resonator had a diameter of 3.6 mm, corresponding to a free-spectral range (FSR) of 18.9 GHz at the experimental wavelength, and was mounted inside a custom-made housing in order to reduce both thermal and mechanical fluctuations, and in order to protect it from dust and humidity. The QCL was free-beam coupled to the resonator through a coupling prism, placed close to the resonator surface. By acting on the temperature, it was possible to tune both the mode width and resonance frequency, in order to select the best coupling condition. Optimal coupling required a beam waist of about 10 mm (radius at  $1/e^2$  of the total beam power). In operating conditions, the measured WGMR transmission mode was 3.1 MHz FWHM, corresponding to a  $Q \approx 2.2 \cdot 10^7$ . The measured value for the Q-factor is in agreement with other measurements made on similar WGMRs at the same working wavelengths.<sup>31,32</sup>

The improvement in terms of frequency stability and linewidth was studied by measuring the laser frequency noise power spectral density (FNPSD) by means of a frequency-to-amplitude converter (fig. 5). In our setup, the converter is the side of a strong CO<sub>2</sub> absorption line, the (000-001) P(42) transition occurring at  $2311.105 \text{ cm}^{-1}$ , with a linestrength of  $4.75 \cdot 10^{-19} \text{ cm}$  (HITRAN units). The CO<sub>2</sub> pressure inside the cell was chosen in order to maximize the slope of the absorption line ( $P \approx 1 \text{ mbar}$ ) for an optimal frequency-to-amplitude conversion. The measured laser FNPSD is shown in fig. 7. The locking bandwidth exceeds 100 kHz and the loop is able to pull down the laser FNPSD by more than 3 orders of magnitude with respect to the free-running laser (black trace). We inferred  $\approx 700 \text{ kHz}$  linewidth for the free-running laser (1 second timescale), which is reduced to 15 kHz in the locked regime (10 kHz for 1 ms timescale).<sup>32</sup> This stability at long timescales marks the difference with respect to previous results on QCLs locked to mid-IR cavities,<sup>33</sup> which suffer of a larger sensibility to external acoustical and mechanical noise. It is interesting to note that the achieved noise reduction is very similar for both the electronic and optical locking, allowing to choose among the two techniques according to the experimental necessities without degradation of the final result.

A test of the suitability of the QCL-WGMR system for high-resolution spectroscopy was performed.<sup>34</sup> In this test a standard pump-probe setup for sub-Doppler spectroscopy was realized. In locking conditions, the QCL was tuned on the same strong CO<sub>2</sub> transition mentioned above. A Lamb dip with about 2 MHz FWHM was recorded, where the main width contribution due to residual Doppler broadening. An uncertainty of 9 kHz on the transition center frequency was obtained, corresponding to a relative precision of about  $10^{-10}$  over a few seconds acquisition time.

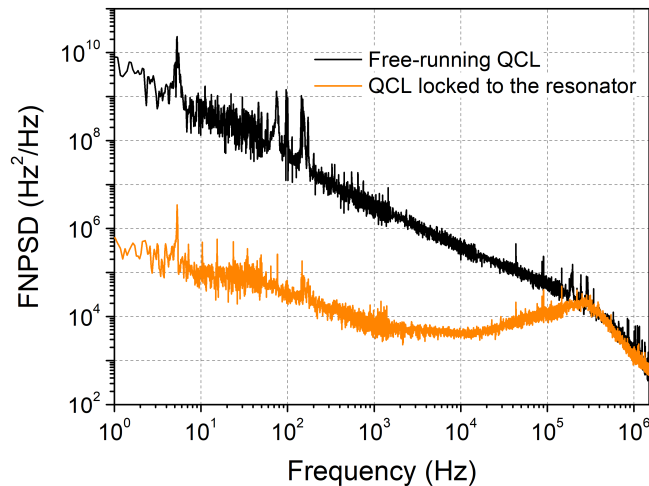


Figure 5. Frequency-noise power spectral density for free-running (black trace) and locked (orange trace) QCL. The frequency cut-off around 300 kHz is due to the limited bandwidth of the detector. Reprinted with permission from [31], copyright 2016.

## 2.2 Mid-infrared frequency combs generation and control

Considering the wide spectral features characterizing molecules in the mid infrared, it's clear that it is very interesting and useful to have OFCs operating directly in this spectral region. Firstly they can serve as direct references for single-frequency MIR lasers, such as DFB QCLs. Even further, they can be used directly for MIR spectroscopy. An OFC radiation can give more spectroscopy information at a time than a single-frequency one, thanks to its instantaneous

spectral coverage. In order to perform high-sensitivity and resolution spectroscopy, it is again fundamental to have intense and narrow (low-frequency-noise) radiation. Moreover, if also a high accuracy is required, an absolute reference is again needed. Pulsed mode-locked lasers have not yet been developed in the MIR, but their NIR spectra can be transferred to the MIR region (MIR-combs) taking advantage of non-linear frequency mixing. A promising alternative is represented by QCLs (QCL-combs).<sup>36</sup> An experiment where a QCL-comb is phase-locked through a single chain to a DFG-comb is here presented. This attempt is aimed both at the stabilization and at the further study of the coherence of the QCL-comb radiation.

### 2.2.1 Quantum-cascade-laser frequency comb stabilization

Several experiments have already proven the intrinsic coherence of the emission of QCL-combs,<sup>37,38</sup> but to be used for high-resolution spectroscopy applications a proper stabilization to overcome technical noise is required. Indeed, for metrological purposes, a fine control of the main optical parameters is required.<sup>39</sup> Moreover, this is an additional occasion for studying the coherence properties of QCL-combs emission. In the following experiment, a DFG-comb has been used to investigate the comb properties of the multimodal QCL emission, in a dual-comb-like setup.<sup>40</sup> This characterization is essential for metrological applications of such QCL-combs. Basically a QCL-comb tooth has been phase-locked to a DFG-comb one and the collective effect on the other QCL-comb teeth has been studied. The results are interpreted within the framework of frequency combs in terms of offset and spacing frequencies, relating these parameters and their fluctuations to primary physics quantities such as the QCL effective waveguide refractive index and the group refractive index.

In fig. 6 the experimental setup is shown. The QCL-comb, provided by ETH Zürich, is a broad-gain Fabry-Pérot device, emitting continuous-wave radiation around 4.70  $\mu\text{m}$ . The spacing (fs) between the longitudinal modes (QCL-comb teeth) is about 7 GHz. The laser working temperature is 16.5°C and the current is 735 mA, with an emitted power of 60 mW on a single transverse mode. The DFG-comb is essentially used to convert the MIR QCL-comb spectrum down to the radio frequencies (RF).

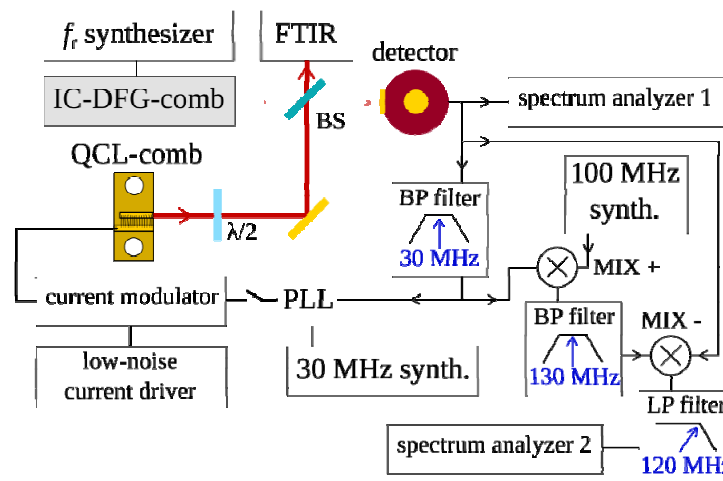


Figure 6. Experimental setup used for the beat-note detection.  $\lambda/2$ : half-wave plate to adjust the polarization; BS: asymmetric non-polarizing beam splitter (transmission 99%, reflection 1%); BP: RF band pass filter (in figure the center frequency is reported); LP: low pass filter; MIX: RF mixer; PLL: phase-locked-loop electronics. Each frequency synthesizer in the setup (including the ones in spectrum analyzers) is referenced to a quartz/Rb/GPS disciplined clock. Reprinted with permission from [40], copyright 2016.

It is important to remark here that the frequency noise of the DFG-comb (single tooth linewidth) is particularly low (2-kHz linewidth on a 1-s time scale). Moreover, the DFG-comb long term frequency stability and frequency accuracy descends directly from the ones of the metrological NIR-comb involved in the generation chain. The DFG-comb repetition rate ( $f_r$ ) is 1 GHz and the spectrum is about 300-GHz wide. As shown in fig. 6, the QCL-comb beam (about 1 mW of power) is superimposed to the DFG-comb beam (about 0.5 mW of power), sending them to a HgCdTe photodetector (200-MHz bandwidth). The recorded heterodyne beat-note signal (HBNS) is used for further analysis of

the phase noise and frequency control of the QCL-comb. A fraction of the HBNS signal is recorded by an RF spectrum analyzer. When the frequency spacing between the QCL-comb modes and the DFG-comb ones falls within the bandwidth of the detector, the obtained RF spectrum is made of several peaks, each of them resulting from the beating between a QCL-comb tooth and a DFG-comb tooth (in a ratio of one every seven). The spacing between these peaks is  $|f_s - 7f_r|$  (about 10 MHz). The HBNS is also used in an RF chain. The signal is filtered at 30 MHz just to select only one peak (with all the parameters chosen to have the better signal-to-noise ratio). Then it is sent to a home-made hybrid analog/digital phase-locked-loop (PLL) electronics. When the loop is closed on the QCL current modulator, this signal is locked to the 30 MHz local oscillator, essentially locking one QCL-comb tooth to a DFG-comb one.

When the QCL-comb operates in free-running regime, the peaks in the HBNS are about 1-MHz wide. As a first step the performance of the loop has been tested. Once closed the loop and optimized the PLL parameters, the HBNS has been acquired with the spectrum analyzer in real-time mode. Each acquisition is made of 20 frames. Each frame contains the HBNS in time domain over a 2-ms time interval sampled at 75 MHz. Afterwards, for each frame the Fourier transform of the signal (amplitude and phase) has been computed.

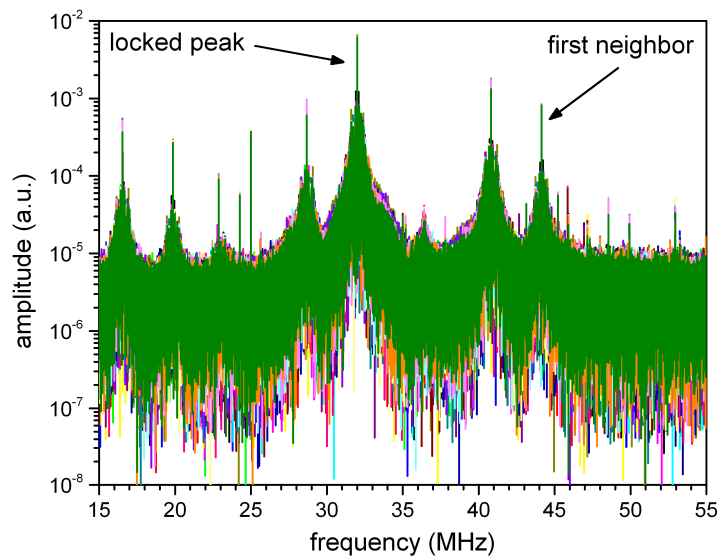


Figure 7. FFT amplitude of the 20 frames of an acquisition of the HBNS. Each color is related to a specific frame. The QCL-comb operates in locking condition. Each frame contains the HBNS in time domain over a 2-ms time interval sampled at 75 MHz. Reprinted with permission from [40], copyright 2016.

All the 20 obtained amplitude spectra of an acquisition are reported in fig. 7. In fig. 8 a zoom of the locked peak (the one filtered to be used in the locking chain) is shown. On a frequency span of 2 MHz the typical shape of locked signals is evident, with the bumps given by the electronic bandwidths. On a span of 12 kHz the peak is still resolution-bandwidth-limited and a perfect stability over the whole acquisition is observed. In fig. 8 the phase of the signal around the locked peak is also reported. The phase is clearly stable over the whole acquisition.

Now, for studying the collective effect of the locking, we concentrate our attention on the other peaks. In fig. 9 a zoom of the first-neighbor peak is shown. On a span of 2 MHz the peak shows a shape close to the one of the locked peak, but on a span of 12 kHz frequency fluctuations are evident.

This experiment proves that the QCL-comb mode used in the locking chain is perfectly stabilized, while the other modes are only partially stabilized. The locked QCL-comb mode shows a perfectly stable phase difference compared to the DFG-comb one, while the other QCL-comb modes show a reduced linewidth from 500 kHz down to values ranging from 1 to 23 kHz on a 40 ms time scale, depending on the distance from the locked mode. Another actuator to control the spacing fluctuations is required in order to lock all the modes. Apparently, the spacing fluctuations are not affected by the locking.

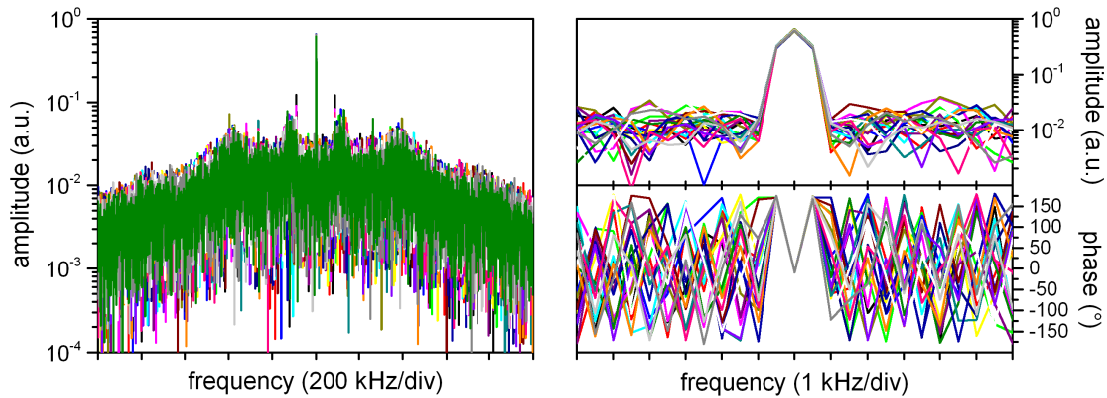


Figure 8. Zoom of the locked peak: amplitude (on two different spans) and phase. Even on the narrower span a perfect stability both of the peak amplitude and phase can be observed. Reprinted with permission from [40], copyright 2016.

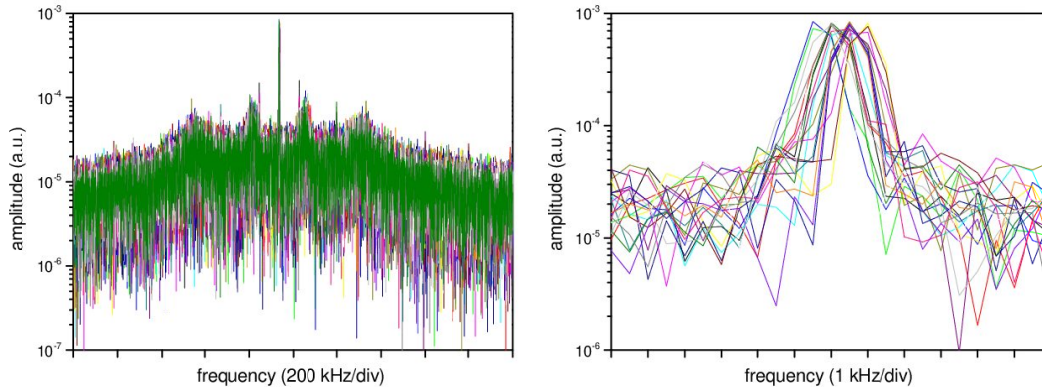


Figure 9. Zoom of the first-neighbor peak in locking operation. On the narrower span the presence of frequency fluctuations is evident. Reprinted with permission from [40], copyright 2016.

### 3. THZ QCLS

#### 3.1 Far-IR domain

The so-called terahertz spectrum, also known as far-IR, conventionally spans the frequency range from 0.1 to 10 THz, corresponding to the wavelength interval from 30 to 3000  $\mu\text{m}$  wavelength. Historically this region is known as ‘terahertz gap’, due to the lack of sufficiently strong and compact sources and sensitive detectors.<sup>41</sup> One of the oldest applications of terahertz radiation is spectroscopy. Many chemical species have indeed very strong characteristic rotational and vibrational absorption lines in the THz range, whose absorption strengths are  $10^3$ – $10^6$  stronger than in the microwave region. Since THz transitions represent a useful molecular ‘signature’, astronomy and space science have recently moved to THz technology.<sup>42</sup> As a topical example, one-half of the total luminosity of the galaxy and 98% of the photons emitted since the Big Bang fall into the terahertz gap.<sup>43</sup>

Much of this radiation is emitted by cool interstellar dust inside our and other galaxies, and thus the study of the discrete lines emitted by light molecular species can give nice insight into star formation and decay, despite the clear need of satellite platforms or high altitudes, due to the strong atmospheric absorption resulting from pressure broadened water and oxygen lines. Furthermore, terahertz thermal emission from gases in the stratosphere and upper troposphere such as water, oxygen, chlorine and nitrogen compounds is useful for the study of chemical processes related to ozone depletion,

pollution monitoring and global warming.<sup>44</sup> Other spectroscopic applications include plasma fusion diagnostics,<sup>45</sup> or identification of different crystalline polymorphic states of a drug.

The lack of coherent sources in this range was first filled by optically pumped fixed-frequency FIR lasers, at the basis of laser magnetic resonance (LMR) spectrometers, having a wider tunability, but only working on paramagnetic species (see e.g. ref. 46). Generation of microwave sidebands on the strongest FIR laser lines in Schottky diodes could produce tunable FIR radiation up to about 3 THz ( $100\text{ cm}^{-1}$ ).<sup>47,48</sup> Continuous spectral coverage from 300 GHz up to about 9 THz was achieved by different configurations based on nonlinear mixing of microwaves with infrared radiation from carbon-dioxide lasers in metal–insulator–metal (MIM) diodes.<sup>49–51</sup> The unique combination of very wide tunability, few tens of kHz frequency uncertainty and kHz level linewidth produced plenty of accurate frequency measurements of atomic and molecular transitions (see e.g. ref. 52–54). A pioneering ‘hybrid’ approach, generating far-IR radiation by mixing, onto a MIM diode, a frequency-locked CO<sub>2</sub> laser and a QCL emitting around 8  $\mu\text{m}$  wavelength, allowed tunable spectroscopy of rotational lines of hydrogen bromide.<sup>55</sup>

### 3.2 Single frequency THz QCLs

The equipment discussed up to now, available for THz generation, is generally bulky, expensive and often suffers from low output powers ( $< \mu\text{W}$ ). Consequently, availability of a new generation of compact, reliable THz sources is the key for the development of the largely underdeveloped THz range. As discussed in the following, THz emitting QCLs are proving to be good candidates to fill this gap. The first report on a THz QCL<sup>56</sup> exploited a careful design of the active region based on a chirped superlattice and an asymmetric low-loss waveguide and emission at 4.4 THz was achieved. In this first experiment, the miniband width was kept lower than the optical phonon energy, in order to avoid photon re-absorption. Since then, despite the cryogenic operation temperatures (199 K),<sup>57</sup> THz QCLs have attracted considerable attention thanks to the high output power ( $> 100\text{ mW}$ ), spectral purity, stability, compactness and reliability, and have now a realistic chance of making a deep impact on technological applications. In fact frequency- and phase-stabilized, high-power and reliable solid-state terahertz sources can indeed find application in a large number of fields, from far-infrared astronomy<sup>58</sup> and high-precision molecular gas spectroscopy<sup>59</sup> to high-resolution coherent imaging and telecommunications.<sup>60,61</sup>

In addressing such application requirements, high frequency stability sources are almost mandatory. In this context, knowledge about the intrinsic linewidth due to quantum noise is key, as it ultimately determines the achievable spectral resolution and coherence length. Environmental effects such as temperature, bias-current fluctuations and mechanical oscillations are widely known to have a significant effect on emission linewidths in QCLs. This means that any experimental linewidth measurement is dominated by extrinsic noise.<sup>62–66</sup> Up to 2012 only a few experimental studies had indeed been reported on the spectral purity of terahertz QCLs, and these give upper limits of 30 kHz, 20 kHz and 6.3 kHz for the instantaneous linewidth.<sup>62,65,66</sup> Environmental effects can be minimized by using frequency-stabilization or phase-locking techniques, resulting in narrower linewidths that are limited by the loop bandwidth of the specific experimental system.<sup>63</sup>

### 3.3 Intrinsic linewidth

Recently, the spectral purity of a THz QCL has been investigated via the measurement of its frequency-noise power spectral density (FNPSD), providing an experimental evaluation and a theoretical assessment of its intrinsic LW.<sup>67</sup> Intensity measurements were performed to retrieve information in the frequency domain by converting the laser frequency fluctuations into detectable intensity (amplitude) variations. As a discriminator, the side of a Doppler-broadened methanol molecular transition has been used. Specifically, the ro-vibrational molecular transition line of CH<sub>3</sub>OH, centered at 2.5227816 THz, was used as a discriminator. Given the intrinsic low-noise nature of the measurement, the converter (or discriminator) must introduce negligible noise providing, at the same time, a gain factor suitable for good detection. A schematic diagram of the experimental set-up used is shown in figure 10.

The collimated THz QCL beam is sent to the gas cell for spectroscopy experiments. It is then split by a wire grid polarizer: the reflected beam is chopped and sent to a pyroelectric detector for the acquisition of the line profile and for frequency stabilization; the transmitted beam is acquired by means of two detectors (a silicon bolometer and a hot-electron bolometer (HEB), depending on the required bandwidth) and used for the frequency-noise measurement. It is worth noting that the gas cell window has been properly tilted with the specific purpose to avoid any optical feedback effect on the measured frequency noise.

During the frequency-noise measurement, the QCL frequency needs to be locked at the half-height position of the absorption line, in order to keep the conversion factor constant at its maximum value. The latter procedure was done by implementing a software PI loop on the QCL current and by using the line around the locking point as a feedback signal. This allows for efficient stabilization of the mean QCL frequency at the right point, without affecting the QCL frequency noise above 10 Hz.

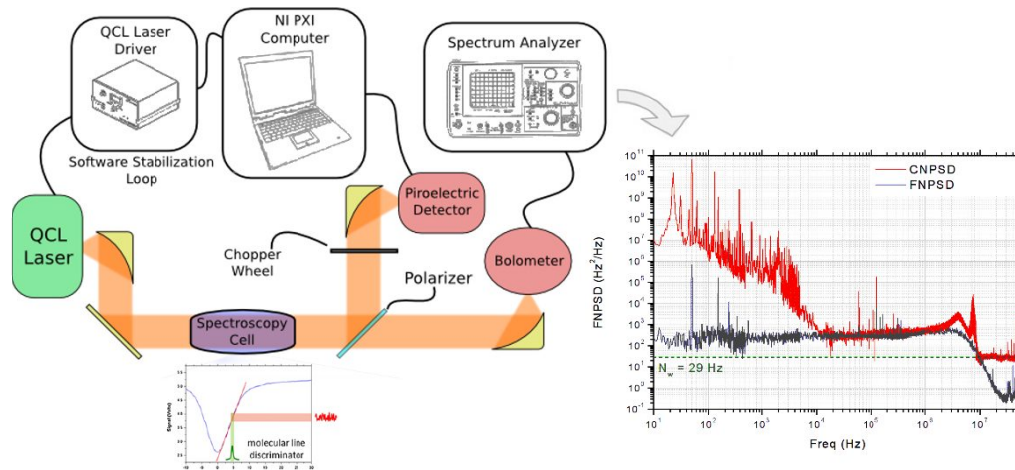


Figure 10. Left: schematic diagram of the experimental set-up, where the function of the molecular line acting as frequency-to-amplitude discriminator is shown. Right: experimental FNPSP of the THz QCL (red trace), compared with the contribution to frequency noise of the CNPSP of the current driver (black trace). The dashed line marks the white noise level. Reprinted with permission from [67], copyright 2012.

The combination of the large detection bandwidth of the HEB with the low-noise fast-Fourier-transform acquisition, enables spectral measurements spanning over seven frequency decades (from 10 Hz to 100 MHz) and 10 amplitude decades. A measurement of the residual amplitude noise is also performed, by shifting the QCL frequency out of the discriminator side. The latter is then subtracted from the former, in order to retrieve the correct FNPSP. The full spectrum of the QCL was obtained by sticking together several acquisitions taken in smaller spectral windows, in order to ensure a high overall resolution. The resulting FNPSP spectrum is plotted in figure 10 inset, together with the current-noise power spectral density (CNPSP) of the current driver, converted to the same units by using the current tuning coefficient. Residual external noise gives rise to the sharp peaks visible throughout the trace. Three distinct domains can be clearly recognized in: (i) the  $f = 10 \text{ Hz}^{-10} \text{ kHz}$  range, where the FNPSP is dominated by a noise not arising from the current driver and therefore ascribed to the QCL itself. The excess frequency noise, with respect to the CNPSP level, that is absent at larger frequencies, can be attributed to spurious low-frequency background radiation signals and/or electronic noise, together with electric field fluctuations due to gain Stark shift and to cavity mode pulling; (ii) the 10 kHz–5 MHz range where the FNPSP is fully dominated by the contribution of the current driver; (iii) above 8 MHz, where an asymptotic flattening is observed in the FNPSP, with a significant deviation from CNPSP, thus suggesting a flattening to a white noise level, therefore leading to an intrinsic LW of  $90 \pm 30 \text{ Hz}$ . Later the same year this astonishing result has been confirmed by an independent study conducted using a Near-infrared Frequency Comb;<sup>68</sup> these results further qualify THz QCLs as ideal metrological sources.

### 3.4 Metrological grade THz QCLs

From this perspective, the development of a metrological referencing technique is very promising in order to fully exploit these devices potentialities. In analogy with other well developed spectral regions, multiple approaches have been tried to migrate the qualities of frequency comb synthesizers (FCSs) to the terahertz region. In a few cases, a link between a continuous wave (CW) terahertz source and a near infrared comb has been provided by detection techniques based on photo-conductive antennas<sup>69</sup> or electro-optic crystals.<sup>70</sup> To detect and phase-lock the beat note, both these techniques involve the CW terahertz source in a low-efficiency up-conversion process. As a consequence, the CW-source power used for the phase-lock is larger than 1 mW. Such limitations have been recently overcome by producing a free-space terahertz FCS and by directly beating it with the CW terahertz source on a square-law detector.<sup>71</sup> This

experimental configuration allows independent optimization of the source and reference figures of merit, for an efficient beat-note detection. Once an appropriate detector is used, the amount of power needed for the frequency control of the terahertz source can be dramatically reduced, while making almost the whole power available for the experiment.

The principle of the THz comb beating with the THz QCL is sketched in figure 11. An optical rectification, in Cherenkov configuration, of a femtosecond mode-locked Ti:Sa laser occurs in a single-mode waveguide fabricated on a MgO-doped LiNbO<sub>3</sub> crystal plate. The generated radiation is a train of THz pulses, each consisting of a single electric field cycle carrying a very large spectral content (from 100 GHz up to 6 THz, centered at 1.6 THz). Since the pulses are identical, the comb-like spectrum of the infinite train has a perfectly zero offset, and a spacing corresponding to the 77.47 MHz repetition rate of the pump laser. Stability in the mHz range was obtained for the repetition rate, thus ensuring stability of each tooth of the THz comb at the 100 Hz level. The generation efficiency is sufficiently high to allow using a very simple setup and a commercial hot-electron-bolometer detector, with 250 MHz bandwidth, to directly observe the beating between single teeth of the comb and a small power fraction (100 nW) from the THz QCL.

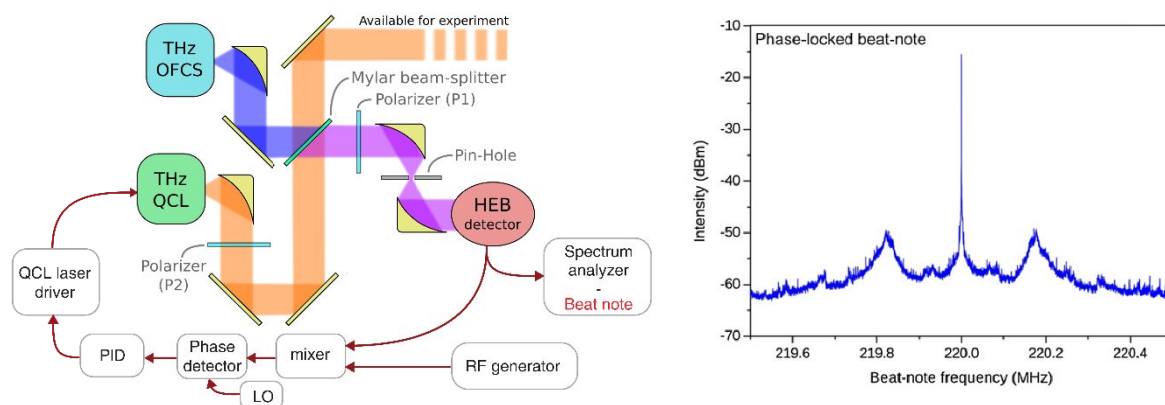


Figure 11: Left The beating between the QCL and the FCS is detected on a HEB. The two beams are superimposed by means of a highly asymmetrical beam splitter, so that more than 99.5% of the QCL radiation is available for the experiment beam. The P1 polarizer ensures polarization matching between the beams, whereas P2 selects the amount of QCL power to be sent to the HEB. A sketch of the electronic setup is given in the lower part of the panel. Right: beat-note spectrum when the QCL is phase-locked to the comb tooth. Reprinted with permission from [71], copyright 2012.

To effectively stabilize the phase of the QCL emission to the frequency comb reference, a phase-lock loop (PLL) needs to be implemented. The simplified scheme of the electronic setup used for closing the PLL is given in fig. 11. The beat-note signal is mixed with a synthesized fixed frequency and processed by an analog/digital phase detector. The correction signal closes the PLL on the fast (1 MHz bandwidth) modulation input of a low-noise QCL current driver (PPQ Sense QubeCL). Locked beat-note spectrum is shown in the right part of fig. 11. The electronic bandwidth of the loop is about 200 kHz, and the achieved signal-to-noise ratio is > 50 dB at 1 Hz RBW, close to the expected limit of 60 dB. By numerical integration of the beat-note spectra, we find that about 75% of the QCL power is phase-locked to the FCS emission. The phase-lock leads to a narrowing of most of the CW laser emission down to the terahertz comb tooth linewidth.

Exploitations of such a system for THz-comb-assisted spectroscopy has already provided new precise results for rotational molecular transitions.<sup>17</sup> In this experiment a direct-absorption spectroscopy setup has been implemented on a 10-cm-long cell filled with methanol gas, using the available fraction of the QCL beam (more than 99% of the total power) and a room-temperature pyroelectric detector, together with an optical chopper on the beam and a lock-in acquisition. Once the investigated transition has been identified on a molecular database, the spectrometer can now be used for accurate measurements of the absolute frequency of the identified lines. To this purpose, the line center, as well as other characteristic parameters, are determined by fitting a Voigt function to a set of experimental spectra taken at different pressures, see fig. 12. The flat residual plot shown in the bottom panel of the figure confirms the good agreement between the fitting curve and the recorded spectrum, and gives a signal-to-noise ratio (SNR) higher than 200.

From the SNR and the linewidth of each Voigt profile (falling in the MHz range and depending on pressure), the statistical error for the fitted line-center frequency is retrieved. It ranges from 30 to 40 kHz (depending on the data set), and it is slightly larger than the error given by the fit routine on the line center ( $\nu_c$ ) parameter, thus better taking into account other error sources, such as the uncertainty on pressure. The linear dependence on pressure of the line-center frequency is shown in fig. 12(b). A pressure shift of about 240 kHz/mbar is measured and, by extrapolating the  $\nu_c$  value at zero pressure, the line-center absolute frequency is retrieved:  $\nu_{c0} = 2553830.766(10)$  MHz. The 10-kHz error, given by the linear fit, corresponds to a  $4 \times 10^{-9}$  relative uncertainty that is about 2 orders of magnitude worse than the accuracy of the THz comb. Indeed, the measurement is limited by the signal-to-noise ratio of the Doppler-limited spectroscopic resolution.

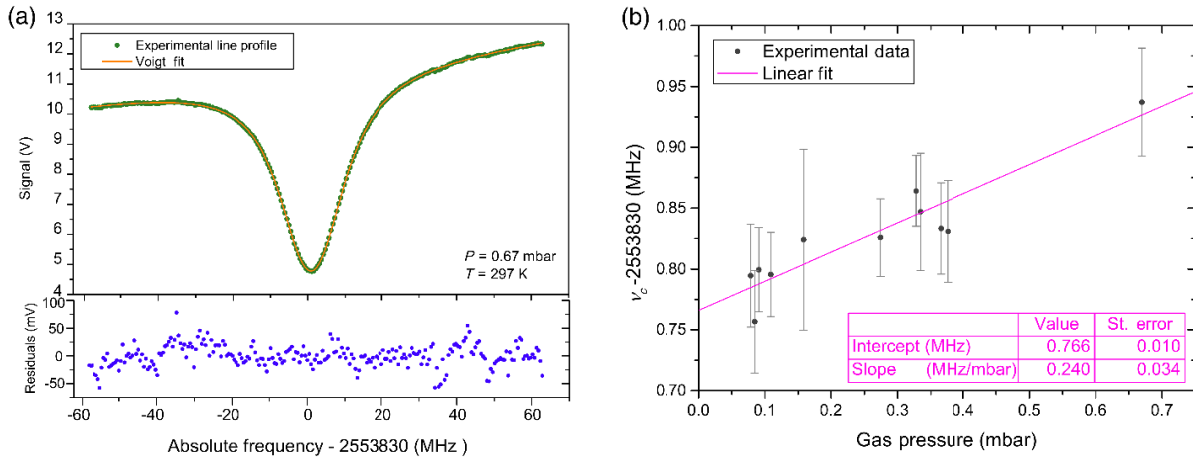


Figure 12. (a) Experimental absorption profile (green dots) and Voigt function fit (red line) with residuals (blue dots, bottom panel), for the investigated line. Gas pressure and temperature during the acquisition are also reported. (b) Dependence of the centerline frequency on gas pressure (black dots), with the corresponding linear fit (purple line). The intercept and the slope values of the fit give the absolute frequency ( $\nu_{c0}$ ) and the pressure shift of the considered line. Reprinted with permission from [17], copyright 2014.

### 3.5 A new generation of room-temperature THz QCLs

As described in the previous paragraph, despite the progress undergone by THz QCLs, the onset of temperature-activated longitudinal optical phonon scattering of electrons in the upper laser state, combined with the difficulty of achieving selective electron injection into the closely spaced laser states, still limits the operation of the best THz QCLs to temperatures of  $\sim 200$  K<sup>57</sup> in pulsed mode. However, RT operation is highly desired for applications and largely simplifies any experimental setup. To address the need for RT THz sources, an alternative approach has been implemented on the basis of intracavity difference-frequency generation (DFG) in mid-IR QCLs.<sup>72,73</sup> With the introduction of a Cherenkov phase-matching scheme for efficient THz extraction,<sup>74,75</sup> THz DFG-QCLs have made marked progress in the past 5 years.<sup>76,77</sup> This foundational approach has several appealing aspects: Because the intersubband transitions within the QCL material itself provide the second order nonlinearity, the sources are monolithic and can be operated at RT, similar to other mid-IRQCLs; in addition, wide THz tunability can be obtained with only modest tuning of the mid-IR modes.<sup>78-81</sup> Depending on the mid-IR pump spacing, THz emission can be varied in the entire 1- to 6-THz range and beyond,<sup>79-80</sup> with limitations set only by the material losses and reduction of THz DFG efficiency.<sup>82</sup> Apart from low-resolution ( $\sim 4$  GHz) Fourier transform infrared (FTIR) spectrometers, in order to establish whether THz DFG-QCLs are a viable alternative to THz QCLs for numerous applications that require narrow-LW emitters, a through characterization of these devices needs to be performed. These has been very recently presented in<sup>83</sup>.

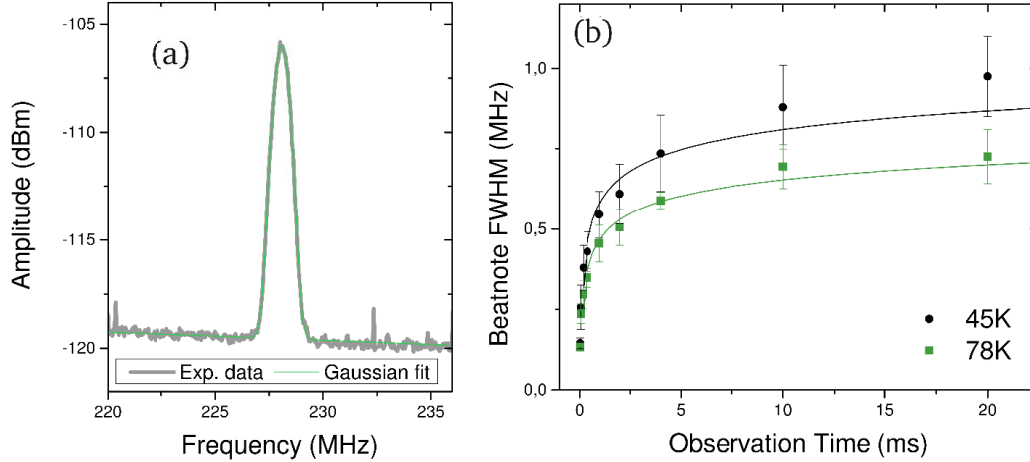


Figure 13: (a) Typical beat note spectrum observed on a spectrum analyzer for 2-ms integration time. (b) Width of the beat note at different time scales measured at two different operating temperatures of the device. The use of an FFT spectrum analyzer allows retrieval of the beat note spectra over different integration times and therefore evaluation of the THz DFG-QCL emission LW at different time scales (ranging from 20 ms to approximately 20 ms). Solid lines are fits using a logarithmic function. Reprinted with permission from [83], copyright 2017.

To probe the LW of the THz emission from the device, we investigated the beat note signal arising from the beating between the THz emission from the DFG-QCL and the free-space THz FCS. The experimental setup is similar to the one shown in fig. 11. The detected beat note spectrum, shown in in fig. 13(a) can be described by a Gaussian function, whose profile has been used to fit each line shape. Because the LW of the THz comb tooth involved in the beating process ( $\sim 130$  Hz at 1 s, as experimentally demonstrated) (11, 15) is negligible with respect to the DFG-QCL THz emission LW, the full width at half maximum (FWHM) of the Gaussian profiles provides an accurate quantitative estimation of the THz emission LW of our device. Moreover, the central value of the beat note frequency, as given by the fit, is determined with an uncertainty of about 1 kHz and can be used to retrieve the absolute center frequency of the QCL emission. The LW of the 2.58 THz emission line of the CW-operated device was measured as a function of the observation time  $t$  at two different temperatures (45 and 78 K), as shown in fig. 13(b). The laser was operated with a pump current of 450 mA for both measurements by using an ultralow noise current driver (ppqSense model QubeCL05). The range of analysis is limited at short time scales at 20 ms, corresponding to the acquisition time of the single FFT spectrum in which the beat note width starts to be limited by the resolution bandwidth of the instrument (in this case, 100 kHz). At this time scale, we measure an upper limit of the QCL LW of 125 kHz.

This same setup can be used to continuously monitor the QCL emission frequency, allowing not only to get absolute frequency characterization, but also for tuning parameters retrieval. Fig. 14 shows the temperature (a) and current (b) dependence of the emission frequency of the device.

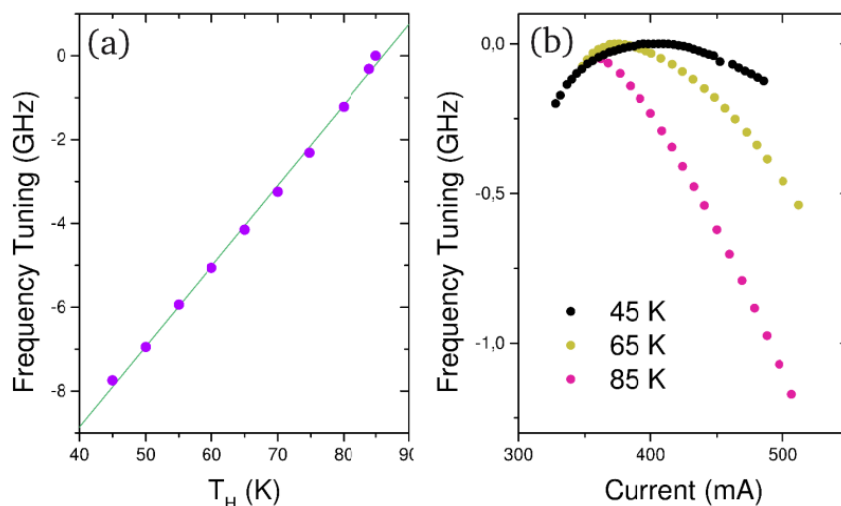


Figure 14: (a) Frequency tuning of the emission line of the DFG-QCL as a function of the QCL operating temperature  $T_H$ , measured while keeping the QCL driving current fixed at 540 mA. (b) QCL frequency tuning as a function of the driving current at different  $T_H$ . Reprinted with permission from [83], copyright 2017.

## REFERENCES

- [1] Kazarinov, R. F. and Suris, R. A., "Possibility of the amplification of electromagnetic waves in a semiconductor with a superlattice," *Sov. Phys. Semicond.* 5(4), 707–709 (1971)
- [2] Cho, A. Y., "Molecular Beam Epitaxy" (Woodbury, NY:AIP) 1997
- [3] Capasso, F., "Band-gap engineering: from physics and materials to new semiconductor devices," *Science* 235 172–6 (1987)
- [4] Faist, J., Capasso, F., Sivco, D. L., Sirtori, C., Hutchinson, A. L. and Cho, A. Y., "Quantum Cascade Laser," *Science* 264(5158), 553–556 (1994)
- [5] Kohler, R., Tredicucci, A., Beltram, F., Beere, H. E., Linfield, E. H., Davies, A. G., Ritchie, D. A., Iotti, R. C. and Rossi, F., "Terahertz semiconductor-heterostructure laser," *Nature* 417 156–9 (2002)
- [6] Capasso, F., "High-performance midinfrared quantum cascade lasers," *Opt. Eng.* 49 111102 (2010)
- [7] Bai, Y., Slivken, S., Kuboya, S., Darvish, S. R. and Razeghi, M., "Quantum cascade lasers that emit more light than heat," *Nature Photon.* 4 99–102 (2010)
- [8] Liu, P. Q., Hoffman, A. J., Escarra, M. D., Franz, K. J., Khurgin, J. B., Dikmelik, Y., Wang, X., Fan, J-Y. and Gmachl, C. F., "Highly power-efficient quantum cascade lasers," *Nature Photon.* 4 95–8 (2010)
- [9] Yao, Y., Hoffman, A. J. and Gmachl, C. F. "Mid-infrared quantum cascade lasers," *Nature Photon.* 6 432–9 (2012)
- [10] Yang, Q., Bronner, W., Manz, C., Moritz, R., Mann, C., Kaufel, G., Kohler, K. and Wagner, J., "Continuous-wave operation of GaInAs–AlGaAsSb quantum cascade lasers," *IEEE Photon. Technol. Lett.* 17 2283–5 (2005)
- [11] Bismuto, A., Riedi, S., Hinkov, B., Beck, M. and Faist, J. "Sb-free quantum cascade lasers in the 3–4  $\mu\text{m}$  spectral range," *Semicond. Sci. Technol.* 27 045013 (2012)
- [12] Williams, B. S., "Terahertz quantum-cascade lasers," *Nature Photon.* 1 517–25 (2007)
- [13] Santamaria, L., Di Sarno, V., De Natale, P., De Rosa, M., Inguscio, M., Mosca, S., Ricciardi, I., Calonico, D., Levi, F. and Maddaloni, P., "Comb-assisted cavity ring-down spectroscopy of a buffer-gas-cooled molecular beam," *Phys. Chem. Chem. Phys.* 18, 16715–16720 (2016)
- [14] Borri, S. and Santambrogio, G., "Laser spectroscopy of cold molecules," *Advances in Physics: X* 1:3, 368–386 (2016).

- [15] Galli, I., Bartalini, S., Ballerini, R., Barucci, M., Cancio, P., De Pas, M., Giusfredi, G., Mazzotti, D., Akikusa, N., and De Natale, P., "Spectroscopic detection of radiocarbon dioxide at parts-per-quadrillion sensitivity," *Optica* 3, 385-388 (2016)
- [16] Giusfredi, G., Bartalini, S., Borri, S., Cancio, P., Galli, I., Mazzotti, D. and De Natale, P., "Saturated-Absorption Cavity Ring-Down Spectroscopy," *Phys. Rev. Lett.* 104, 110801 (2010)
- [17] Bartalini, S., Consolino, L., Cancio, P., De Natale, P., Bartolini, P., Taschin, A., De Pas, M., Beere, H., Ritchie, D., Vitiello, M. S., and Torre, R., "Frequency-Comb-Assisted Terahertz Quantum Cascade Laser Spectroscopy," *Phys. Rev. X* 4, 021006 (2014)
- [18] Cappelli, F., Galli, I., Borri, S., Giusfredi, G., Cancio, P., Mazzotti, D., Montori, A., Akikusa, N., Yamanishi, M., Bartalini, S. and De Natale, P., "Sub-kilohertz linewidth room-temperature mid-IR quantum cascade laser using a molecular sub-Doppler reference," *Opt. Lett.* 37(23), 4811–4813 (2012)
- [19] Mazzotti, D., Cancio, P., Giusfredi, G., De Natale, P. and Prevedelli, M., "Frequency-comb-based absolute frequency measurements in the mid-infrared with a difference-frequency spectrometer," *Opt. Lett.* 30(9), 997–999 (2005)
- [20] Bartalini, S., Borri, S., Galli, I., Giusfredi, G., Mazzotti, D., Edamura, T., Akikusa, N., Yamanishi, M. and De Natale, P., "Measuring frequency noise and intrinsic linewidth of a room-temperature DFB quantum cascade laser," *Opt. Express* 19(19), 17996–18003 (2011)
- [21] Tombez, L., Francesco, J. D., Schilt, S., Domenico, G. D., Faist, J., Thomann, P. and Hofstetter, D., "Frequency noise of free-running 4.6  $\mu\text{m}$  distributed feedback quantum cascade lasers near room temperature," *Opt. Lett.* 36(16), 3109–3111 (2011)
- [22] Maddaloni, P., Bellini, M. and De Natale, P., [Laser-based measurements for time and frequency domain applications: a handbook], CRC Press, 6000 Broken South Parkway NW 300, Boca Raton, FL 33487-2742, USA (2013)
- [23] Foreman, S. M., Marian, A., Ye, J., Petrukhin, E. A., Gubin, M. A., Mücke, O. D., Wong, F. N. C., Ippen, E. P. and Kärtner, F. X., "Demonstration of a HeNe/CH<sub>4</sub>-based optical molecular clock," *Opt. Lett.* 30(5), 570–572 (2005)
- [24] Harvard-Smithsonian Center for Astrophysics (CfA), V. E. Zuev Institute of Atmospheric Optics (IAO), "HITRAN on the Web," <http://hitran.iao.ru/> (2012)
- [25] Galli, I., Cumis, M. S. de, Cappelli, F., Bartalini, S., Mazzotti, D., Borri, S., Montori, A., Akikusa, N., M. Yamanishi, Giusfredi, G., Cancio, P. and De Natale, P., "Comb-assisted subkilohertz linewidth quantum cascade laser for high-precision mid-infrared spectroscopy," *Appl. Phys. Lett.* 102, 121117 (2013)
- [26] Lim, E. J., Hertz, H. M., Bortz, M. L. and Fejer, M. M., "Infrared radiation generated by quasi-phase-matched difference-frequency mixing in a periodically poled lithium niobate waveguide," *Appl. Phys. Lett.* 59(18), 2207–2209 (1991)
- [27] Galli, I., Bartalini, S., Cancio, P., Giusfredi, G., Mazzotti, D. and De Natale, P., "Ultra-stable, widely tunable and absolutely linked mid-IR coherent source," *Opt. Express* 17(12), 9582–9587 (2009)
- [28] Telle, H. R., Lipphardt, B. and Stenger, J., "Kerr-lens, mode-locked lasers as transfer oscillators for optical frequency measurements," *Appl. Phys. B* 74, 1–6 (2002)
- [29] Galli, I., Bartalini, S., Borri, S., Cancio, P., Giusfredi, G., Mazzotti, D. and De Natale, P., "Ti:sapphire laser intracavity difference-frequency generation of 30 mW cw radiation around 4.5  $\mu\text{m}$ ," *Opt. Lett.* 35(21), 3616–3618 (2010)
- [30] Savchenkov, A. A., Matsko, A. B., Ilchenko, V. S., and Maleki, L., "Optical resonators with ten million finesse," *Opt. Express* 15, 6768 (2007)
- [31] Siciliani de Cumis, M., Borri, S., Insero, G., Galli, I., Savchenkov, A., Eliyahu, D., Ilchenko, V., Akikusa, N., Matsko, A., Maleki, L., and De Natale, P., "Microcavity-Stabilized Quantum Cascade Laser", *Laser Photonics Rev.* 10, 153–157 (2016)
- [32] Savchenkov, A. A., Ilchenko, V. S., Di Teodoro, F., Belden, P. M., Lotshaw, W. T., Matsko, A. B., and Maleki, L., "Generation of Kerr combs centered at 4.5  $\mu\text{m}$  in crystalline microresonators pumped with quantum-cascade lasers", *Opt. Lett.* 40, 3468 (2015)
- [33] Lecaplain, C., Javerzac-Galy, C., Gorodetsky, M. L., and Kippenberg, T. J., "Mid-infrared ultra-high-Q resonators based on fluoride crystalline materials", *Nature Comm.* 7, 13383 (2016)
- [34] Fasci, E., Coluccelli, N., Cassinerio, M., Gambetta, A., Hilico, L., Gianfrani, L., Laporta, P., Castrillo, A., and Galzerano, G., "Narrow-linewidth quantum cascade laser at 8.6  $\mu\text{m}$ ", *Opt. Lett.* 39, 4946, (2014)

- [35] Borri, S., Siciliani de Cumis, M., Inero, G., Bartalini, S., Cancio, P., Mazzotti, D., Galli, I., Giusfredi, G., Santambrogio, G., Savchenkov, A., Eliyahu, D., Ilchenko, V., Akikusa, N., Matsko, A., Maleki, L., and De Natale, P., "Tunable Microcavity-Stabilized Quantum Cascade Laser for Mid-IR High-Resolution Spectroscopy and Sensing", *Sensors* 16, 238 (2016)
- [36] Hugi, A., Villares, G., Blaser, S., Liu, H. C. and Faist, J., "Mid-infrared frequency comb based on a quantum cascade laser," *Nature* 492, 229–233 (2012)
- [37] Villares, G., Hugi, A., Blaser, S. and Faist, J., "Dual-comb spectroscopy based on quantum-cascade-laser frequency combs," *Nat. Commun.* 5, 5192 (2014)
- [38] Cappelli, F., Villares, G., Riedi, S. and Faist, J., "Intrinsic linewidth of quantum cascade laser frequency combs," *Optica* 2(10), 836–840 (2015)
- [39] Schilt, S., Bucalovic, N., Dolgovskiy, V., Schori, C., Stumpf, M. C., Di Domenico, G., Pekarek, S., Oehler, A. E. H., Südmeyer, T., Keller, U. and Thomann, P., "Fully stabilized optical frequency comb with sub-radian CEO phase noise from a SESAM-modelocked 1.5- $\mu\text{m}$  solid-state laser," *Opt. Express* 19(24), 24171–24181 (2011)
- [40] Cappelli, F., Campo, G., Galli, I., Giusfredi, G., Bartalini, S., Mazzotti, D., Cancio, P., Borri, S., Hinkov, B., Faist, J. and De Natale, P., "Frequency stability characterization of a quantum cascade laser frequency comb," *Laser Photonics Rev.* 10, 623–630 (2016)
- [41] Consolino, L., Bartalini, S., De Natale, P., "Terahertz Frequency Metrology for Spectroscopic Applications: a Review", *J. Infrared Milli. Terahz. Waves*, 38, 1289-1315 (2017)
- [42] Testi, L., Zwaan, M., Vlahakis, C. and Corder, S., "Science verification datasets on the ALMA science portal", *Messenger* 150 17 (2012)
- [43] Leisawitz, D. T. et al., "Scientific motivation and technology requirements for the SPIRIT and SPECS far-infrared / submillimeter space interferometers", *Proc. SPIE* 4013 36–46 (2000)
- [44] Bellini, M., De Natale, P., Di Lonardo, G., Fusina, L., Inguscio, M. and Prevedelli, M., "Tunable far infrared spectroscopy of 16O3 ozone", *J. Mol. Spectros.* 152 256–9 (1992)
- [45] Luhmann, N. C. and Peebles, W. A., "Instrumentation for magnetically confined fusion plasma diagnostics", *Rev. Sci. Instrum.* 55 279–331 (1984)
- [46] Brown, J. M., Evenson, K. M. and Zink, L., "Laser magnetic-resonance measurement of the 3P1–3P2 fine-structure splittings in 17O and 18O", *Phys. Rev. A* 48 3761–3 (1993)
- [47] Bićanić, D. D., Zuidberg, B. F. J., and Dymanus, A., "Generation of continuously tunable laser sidebands in the submillimeter region", *Appl. Phys. Lett.* 32 367 (1978)
- [48] Farhoomand, J., Blake, G. A., Frerking, M. A. and Pickett, H. M., "Generation of tunable laser sidebands in the far-infrared region", *J. Appl. Phys.* 57 1763 (1985)
- [49] Evenson, K. M., Jennings, D. A. and Petersen, F. R., "Tunable far-infrared spectroscopy", *Appl. Phys. Lett.* 44 576 (1984)
- [50] Zink, L. R., De Natale, P., Pavone, F. S., Prevedelli, M., Evenson, K. M., and Inguscio, M., "Rotational far infrared spectrum of 13CO", *J. Mol. Spectrosc.* 143 304–10 (1990)
- [51] Odashima, H., Zink, L. R. and Evenson, K. M., "Tunable far-infrared spectroscopy extended to 9.1 THz", *Opt. Lett.* 24 406 (1999)
- [52] Bellini, M., De Natale, P., Inguscio, M., Fink, E., Galli, D. and Palla, F., "Laboratory measurements of rotational transitions of lithium hydride in the far-infrared", *Astrophys. J.* 424 507–9 (1994)
- [53] Buffà, G., Tarrini, O., De Natale, P., Inguscio, M., Pavone, F., Prevedelli, M., Evenson, K. M., Zink, L., and Schwaab, G., "Far-infrared self-broadening in methylcyanide: absorber–perturber resonance", *Phys. Rev. A* 45 6443–50 (1992)
- [54] De Natale, P., Bellini, M., Goetz, W., Prevedelli, M. and Inguscio, M., "Hyperfine structure and isotope shift in the far-infrared ground-state transitions of atomic oxygen", *Phys. Rev. A* 48 3757–60 (1993)
- [55] Gagliardi, G., Viciani, S., Inguscio, M., De Natale, P., Gmachl, C. F., Capasso, F., Sivco, D. L., Baillargeon, J. N., Hutchinson, A. L. and Cho, A. Y., "Generation of tunable far-infrared radiation with a quantum cascade laser" *Opt. Lett.* 27 521–3 (2002)
- [56] Kohler, R. et al., "Terahertz semiconductor heterostructure laser", *Nature* 417, 156–159 (2002)
- [57] Fatholouloumi, S., Dupont, E., Chan, C. W. I., Wasilewski, Z. R., Laframboise, S. R., Ban, D., Mátyás, A., Jirauschek, C., Hu, Q. and Liu, H. C., "Terahertz quantum cascade lasers operating up to  $\sim 200$  K with optimized oscillator strength and improved injection tunneling", *Opt. Express* 20 3866 (2012)

- [58] Reix, J.-M. et al., "The Herschel/Planck programme, technical challenges for two science missions, successfully launched", *Acta Astronom.* 34, 130–148 (2009)
- [59] Mittleman, D. M., "Sensing with Terahertz Radiation" (Springer, 2003)
- [60] Tonouchi, M., "Cutting edge terahertz technology", *Nature Photon.* 1, 97–105 (2007)
- [61] Capasso, F. et al., "Quantum cascade lasers: ultrahigh-speed operation, optical wireless communication, narrow linewidth and far-infrared emission", *IEEE J. Quantum Electron.* 38, 511–532 (2002)
- [62] Barkan, A. et al., "Linewidth and tuning characteristics of terahertz quantum cascade lasers", *Opt. Lett.* 29, 575–577 (2004)
- [63] Betz, A. L. et al., "Frequency and phase-lock control of a 3 THz quantum cascade laser", *Opt. Lett.* 30, 1837–1839 (2005)
- [64] Maulini, R. et al., "Continuous-wave operation of a broadly tunable thermoelectrically cooled external cavity quantum cascade-laser", *Opt. Lett.* 30, 2584–2586 (2005)
- [65] Hubers, H. et al., "Terahertz quantum cascade laser as local oscillator in a heterodyne receiver", *Opt. Express* 13, 5890–5896 (2005)
- [66] Baryshev, A. et al., "Phase locking and spectral linewidth of a two-mode terahertz quantum cascade laser", *Appl. Phys. Lett.* 89, 031115 (2006)
- [67] Vitiello, M. S., Consolino, L., Bartolini, S., Taschin, A., Tredicucci, A., Inguscio, M., De Natale, P., "Quantum-limited frequency fluctuations in a terahertz laser", *Nat. Photonics* 6, 525–528 (2012)
- [68] Ravaro, M., Barbieri, S., Santarelli, G., Jagtap, V., Manquest, C., Sirtori, C., Khanna, S. P., and Linfield, E. H., "Measurement of the Intrinsic Linewidth of Terahertz Quantum Cascade Lasers Using a Near-Infrared Frequency Comb", *Opt. Express* 20, 25 654 (2012)
- [69] Ravaro, M. et al., "Phase-locking of a 2.5 THz quantum cascade laser to a frequency comb using a GaAs photomixer", *Opt. Lett.* 36, 3969–3971 (2011)
- [70] Barbieri, S. et al., "Phase-locking of a 2.7-THz quantum cascade laser to a mode-locked erbium-doped fibre laser", *Nat. Photon.* 4, 636–640 (2010)
- [71] Consolino, L., Taschin, A., Bartolini, P., Bartolini, S., Cancio, P., Tredicucci, A., Beere, H. E., Ritchie, D. A., Torre, R., Vitiello, M. S., De Natale, P., "Phase-locking to a free-space terahertz comb for metrological-grade terahertz lasers", *Nat. Commun.* 3, 1040 (2012)
- [72] Belkin, M. A., Capasso, F., Belyanin, A., Sivco, D. L., Cho, A. Y., Oakley, D. C., Vineis, C. J., Turner, G. W., "Terahertz quantum-cascade-laser source based on intracavity difference-frequency generation", *Nat. Photonics* 1, 288–292 (2007)
- [73] Belkin, M. A., Capasso, F., Xie, F., Belyanin, A., Fischer, M., Wittmann, A., Faist, J., "Microwatt-level terahertz intra-cavity difference-frequency generation in mid-infrared quantum cascade lasers", *Appl. Phys. Lett.* 92, 201101 (2008)
- [74] Vijayraghavan, K., Adams, R. W., Vizbaras, A., Jang, M., Grasse, C., Boehm, G., Amann, M. C., Belkin, M. A., "Terahertz sources based on Čerenkov difference-frequency generation in quantum cascade lasers", *Appl. Phys. Lett.* 100, 251104 (2012)
- [75] Vijayraghavan, K., Jiang, Y., Jang, M., Jiang, A., Choutagunta, K., Vizbaras, A., Demmerle, F., Boehm, G., Amann, M. C., Belkin, M. A., "Broadly tunable terahertz generation in mid-infrared quantum cascade lasers", *Nat. Commun.* 4, 2021 (2013)
- [76] Lu, Q., Wu, D., Sengupta, S., Slivken, S., Razeghi, M., "Room temperature continuous wave, monolithic tunable THz sources based on highly efficient mid-infrared quantum cascade lasers", *Sci. Rep.* 6, 23595 (2016)
- [77] Belkin, M. A., Capasso, F., "New frontiers in quantum cascade lasers: High performance room temperature terahertz sources", *Phys. Scr.* 90, 118002 (2015)
- [78] Jung, S., Jiang, A., Jiang, Y., Vijayraghavan, K., Wang, X., Troccoli, M., Belkin, M. A., "Broadly tunable monolithic room-temperature terahertz quantum cascade laser sources", *Nat. Commun.* 5, 4267 (2014)
- [79] Jiang, Y., Vijayraghavan, K., Jung, S., Demmerle, F., Boehm, G., Amann, M. C., Belkin, M. A., "External cavity terahertz quantum cascade laser sources based on intra-cavity frequency mixing with 1.2–5.9 THz tuning range", *J. Opt.* 16, 094002 (2014)
- [80] Jung, S., Jiang, Y., Vijayraghavan, K., Jiang, A., Demmerle, F., Boehm, G., Wang, X., Troccoli, M., Amann, M. C., Belkin, M. A., "Recent progress in widely tunable single-mode room temperature terahertz quantum cascade laser sources", *IEEE J. Sel. Topics Quantum Electron.* 21, 120071 (2015)
- [81] Jiang, A., Jung, S., Jiang, Y., Vijayraghavan, K., H. Kim, J., Belkin, M. A., "Widely tunable terahertz source based on intra-cavity frequency mixing in quantum cascade laser arrays", *Appl. Phys. Lett.* 106, 261107 (2015)

- [82] Jiang, Y., Vijayraghavan, K., Jung, S., Jiang, A., Kim, J. H., Demmerle, F., Boehm, G., Amann, M. C., Belkin, M. A., "Spectroscopic study of terahertz generation in mid-infrared quantum cascade lasers", *Sci. Rep.* 6, 21169 (2016)
- [83] Consolino, L., Jung, S., Campa, A., De Regis, M., Pal, S., Kim, J. H., Fujita, K., Ito, A., Hitaka, M., Bartalini, S., De Natale, P., Belkin, M. A., Vitiello, M. S., "Spectral purity and tenability of terahertz quantum cascade laser sources based on intracavity difference-frequency generation", *Sci. Adv.* 3, e1603317 (2017)